



Experimental Investigation of Environment Temperature Effect on Fatigue of Shape Memory Alloy with Phase Transformation

Israa Nizar Haider

University of Baghdad, College of Engineering
Mechanical Engineering Department, Iraq- Baghdad
israa.haider2003m@coeng.uobaghdad.edu.iq

Prof. Dr. Abdullah Dhayea
Assi

University of Baghdad, College of Engineering
Mechanical Engineering Department, Iraq- Baghdad
drabdullahdhayea@uobaghdad.edu.iq

ABSTRACT

When compared to other materials used in engineering applications, shape-memory alloys (SMAs) are a type of smart material have superior mechanical properties, distinguished by their capacity to return their original shape when heated. At low temperatures, they have low yield strength, facilitating their transformation into any form. The alloy maintains this form until the temperature rises higher than the temperature of their transformation, then return to its original shape. This work studied how lower temperatures affect the tensile and fatigue behavior of SMAs. Both tensile and fatigue testing were conducted using the nickel-rich Nitinol alloy ($Ni_{60}Ti_{30}$). The alloy has phase transformation temperatures as (Austenite finish Temperature= $10^{\circ}C$, Austenite start Temperature= $-2^{\circ}C$, and Martensite start Temperature= $-17^{\circ}C$). The tensile test was performed at three different temperatures ($-20^{\circ}C$, $0^{\circ}C$, and $24^{\circ}C$). The fatigue test was then carried out using a rotary bending fatigue machine with a cooling chamber surrounding the sample to ensure low-temperature conditions. Nitinol Samples with a neck radius of (4 mm) were loaded with different cyclical stresses. Each case's mechanical characteristics changed as a result of the phase shift brought on by the test's low ambient temperature. The fatigue strength (endurance limit) was determined by plotting a stress vs. cycles (S-N) diagram on a logarithmic scale and using the linear relationship to get the fatigue strength. Also, it was shown that external elements such as material dimensions, surface finish, and unsuitable loading caused the experimental number of cycles to differ from the expected number of cycles to failure. ANSYS workbench was used to simulate fatigue testing, and its findings are in good agreement with the results of the experiments.

Keywords:

Shape Memory Alloy (SMA), Fatigue, Nitinol, Phase Transformation

1- Introduction:

Engineers are researching the use of smart materials to create new multifunctional actuator sensor systems that can replace cutting-edge actuators and produce innovative or superior industrial applications and products. Shape memory alloys (SMAs), which can be used to generate movement and force for actuation or quantitative sensor measurements,

are an example of smart or active materials that may change their characteristics in response to external fields. When compared to electric, electromagnetic, hydraulic, or pneumatic actuators, SMAs frequently give very energy-efficient solutions and can reduce weight and structural space because of their high energy and power densities. Moreover, they don't emit any noise or emissions [1,2]. Without a doubt,

Fatigue plays an essential role in all applications of industrial design. Many components are subjected to variable levels of stress/strain, and fatigue could play a role in any of these conditions [3]. Across a wide range of engineering applications, many fatigue designs are required to operate in low-temperature environments. Therefore, it is very necessary to know the mechanical behavior of the materials used in these applications when operated under different temperature conditions [4]. Due to its shape memory effect (SME), super-elasticity, high damping characteristics, resistance characteristics, mechanical properties, compactness, and lightweight, SMA is considered to be a smart alloy. Because of the factors mentioned, NiTi-SMA provides a wide range of use [5,6]. Because of their dependability and flexibility, shape memory materials are getting an increasing variety of applications. They have generated considerable attention in a variety of applications, particularly those in Automobiles, airplanes, medical technology, and civil engineering [7]. For example, the CryoFit coupling tube [8] shown in Fig. 1. is made by machining the SMA

bar. The inside diameter of this connection is somewhat smaller than the exterior diameter of the tubes it is intended to join at room temperature and austenitic conditions. Next, a coupling is filled with liquid nitrogen. At this cryogenic temperature, it transforms into martensitic. The connection is then mechanically expanded by employing a tapered steel mandrel to increase its interior diameter so that it is greater than the tubes' exterior diameter. It has been kept in liquid nitrogen before being given to the customer in this stretched shape. Once it has arrived at the desired position, the coupler is put over the connection between the two tubes. It shrinks down over the tubes with a significant radial force as it tries to restore its original austenitic shape when it warms up [9]. Lifetime prediction of components subjected to a cyclic mechanical motion is essential for the design and optimization of all technical equipment manufactured of Nitinol or other materials. It is possible to assess the durability and safety of these devices by examining their resistance to fracture and fatigue.

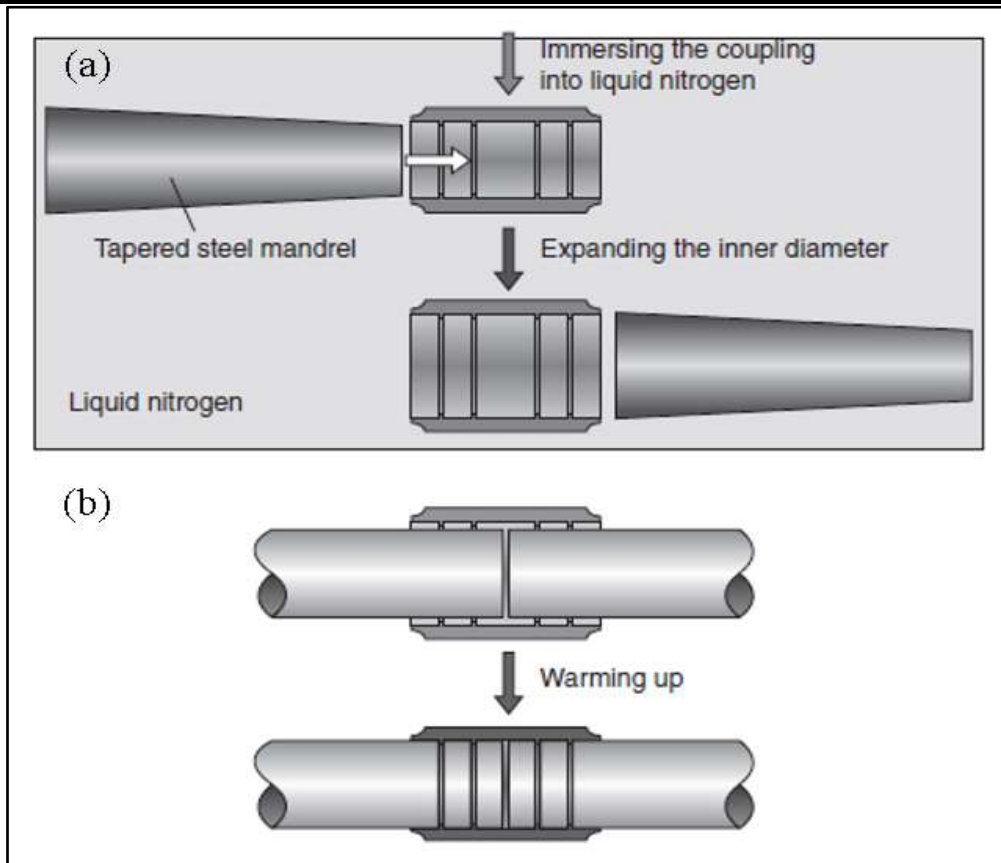


Fig. 1. Schematic diagram of the mechanism of CryoFit: a - The coupling in the liquid nitrogen is in the martensitic phase; b- Coupling positioned over a joint of the two tubes and warming up to shrink [8].

2- The aim of the study:

This study aims to:

- 1- understand the behavior of the Nitinol alloy under the influence of the tensile and fatigue stresses when it is in low-temperature conditions that exceed the limits of the degree of phase transformation of the alloy used in this work.
- 2- compare the effect of tensile and fatigue loads at the different phases of nitinol caused by different environmental temperatures.

3- Materials and methods:

A Ni-rich (nickel-titanium) alloy was used in this work. As it was obtained in the form of a rod with a diameter of 10mm. Phase transformation temperatures for the used alloy were ($A_f=10^{\circ}C$, $A_s=-2^{\circ}C$, and $M_s=-17^{\circ}C$). The chemical composition was examined in order to ascertain the proportions of the alloy, the results are listed in Table (1).

Table 1. The chemical composition of Ni-Ti samples

metal	Ni	Ti	Cu	Fe	Mo	Mn
Weight%	60.7	30.8	3.93	1.12	1.64	0.436

The samples were cold worked into the standard dimensions (ASTM-E8-04) to perform tensile test, which was carried out at three different temperatures ($24^{\circ}C$, $0^{\circ}C$, and $-20^{\circ}C$) to determine the mechanical properties in each

case which are the same cases applied in a fatigue test. The dimensions of the fatigue samples were created to match the test device. Fig. 2. shows the samples' dimensions after being prepared for use in tests.

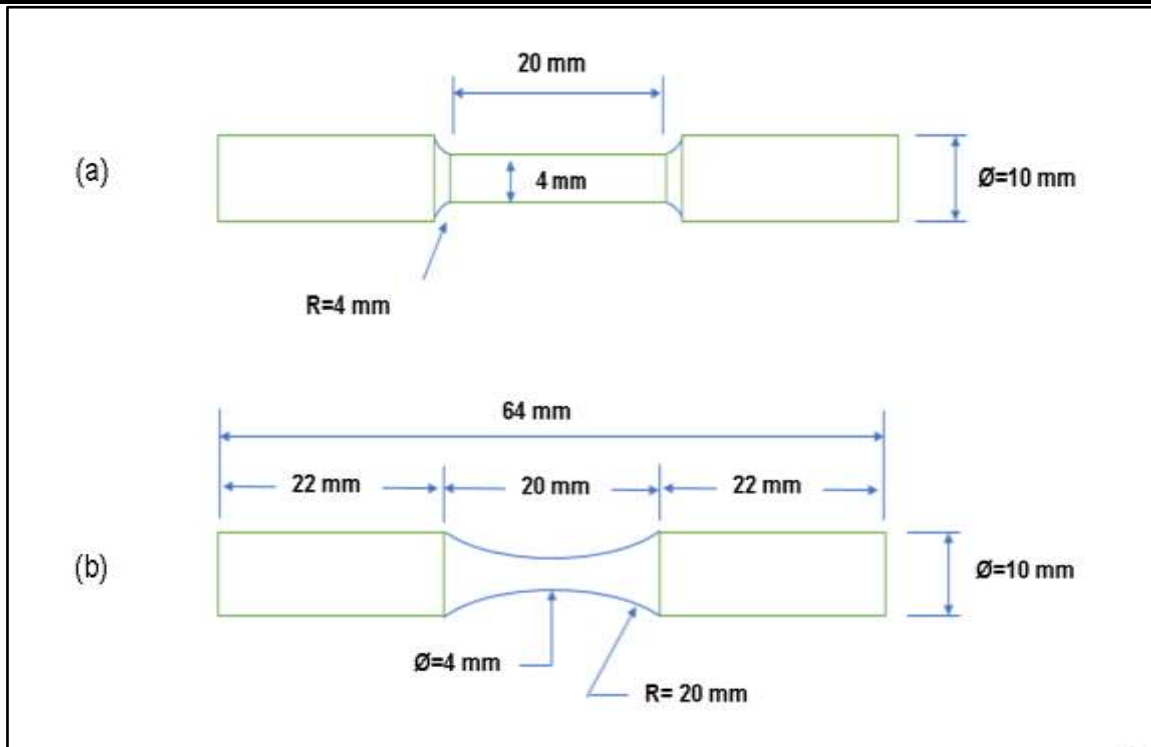


Fig. 2: samples dimensions: a- Tensile test sample; b- Fatigue test sample

High-cycle fatigue testing was performed using a rotary bending fatigue machine of type (HI-TECH LIMITED) with a cooling chamber set up to provide the required temperatures for each test case. The force was applied to the fatigue specimen with a circular cross-section causing a continuous bending moment. When a stationary force was supplied to a rotating specimen, the stress at any point on its outer surface increased from zero to the maximum tension stress, then decreased to the compressive stress leads to stress ratio (R=-1) before returning to zero. Different loads were applied to the samples to provide a different value of bending moment in each experiment. The values of the bending moment were adopted as a proportion of the yield stress that was practically read from the tensile test. The load applied on fatigue apparatus calculated by applying the relation shown below.

$$\sigma_b = \frac{MY}{I} \tag{1}$$

Where:

σ_b : The bending stress (Mpa).

M : The neutral axis moment.

Y : The distance in perpendicular to the neutral axis, ($Y = \frac{d}{2}$)(mm).

I : is the moment of inertia, which is equal to $\frac{\pi d^4}{64}$ (mm⁴).

d : is the specimen's minimum diameter.

$$\sigma_b = \frac{32PL}{\pi D^3} \quad (L: \text{The arm distance of the applied load } P, L=91 \text{ mm})$$

The main part of the cooling chamber is a type of thermoelectric cooler (TEC). When the cooling fins are in operation, one side is cooling and the other releases the heat, working surfaces need to effectively radiate heat. So, a fan had been used to dissipate heat. A temperature Sensor type (NTC 10K) with an accuracy range of 0.05°C to 1.00°C was installed next to the sample within the cooling room to ensure that the temperatures remain consistent during the test. Fig. 3. shows the flowchart of the cooling system.

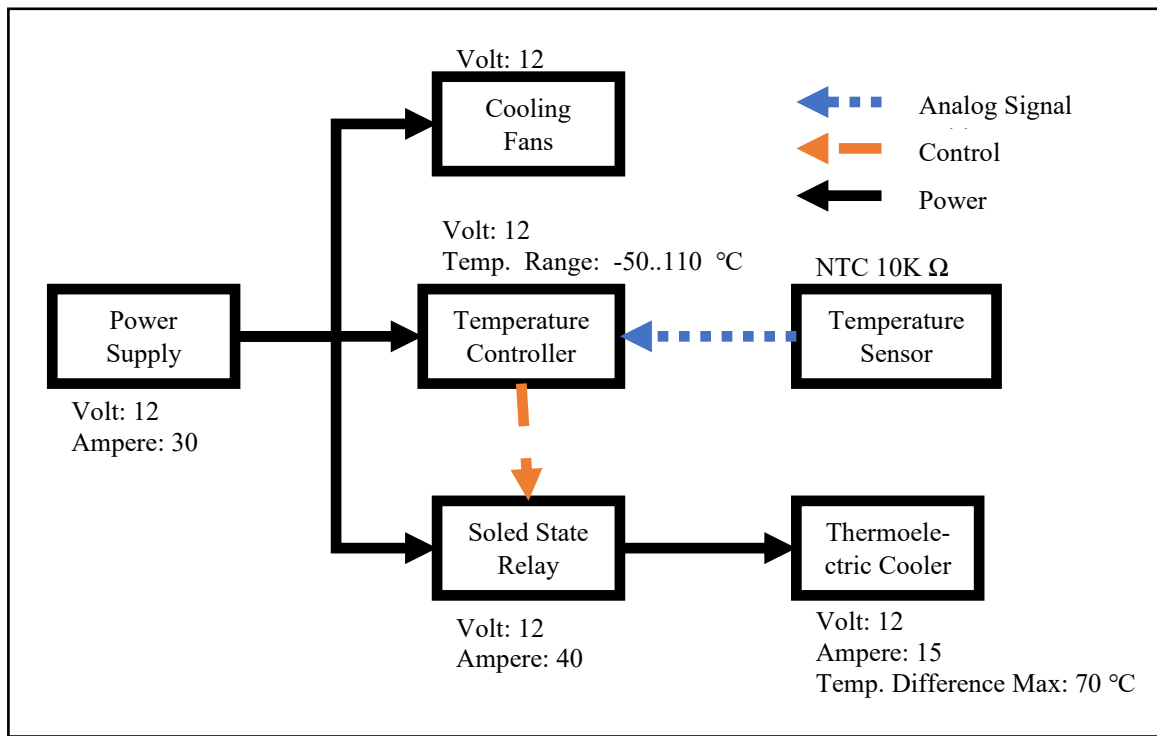


Fig. 3. The cooling system's flowchart.

It was essential to calculate the thermal stress and determine its impact on the value of alternating stress at each experiment because it is expected that the changing the temperature during the fatigue test will result in the occurrence of thermal stress, which will change the expected fatigue life. The thermal stress produced by cooling down determined according to equation (2).

$$\sigma_{th} = \alpha E \Delta T$$

(2)

where α in each case was based on earlier nitinol studies[10], while E is determined by experimental tensile tests. Noting that the expansion that occurs when temperature decreases due to phase transformation will lead to a negative thermal expansion coefficient. For thermomechanical stresses, maximum and minimum stresses were calculated:

$$\sigma_{max} = \sigma_b + \sigma_{th}$$

(3)

$$\sigma_{min} = -\sigma_b + \sigma_{th}$$

(4)

The alternating and mean stresses are expressed as:

$$\sigma_a = \frac{\sigma_{max} - \sigma_{min}}{2}$$

(5)

$$\sigma_m = \frac{\sigma_{max} + \sigma_{min}}{2}$$

(6)

The theory of distortion energy failure was proved to be an effective way to convert the various stresses acting on a ductile material's stress element into a single equivalent von Mises stress. Here, we're going to utilize the same technique because there is combination of loadings, including bending and thermal stress which considered as an axial stress. Taking into consideration that there is no torsional stress [11].

$$\sigma'_a = \left\{ \left[(K_f)_{bending} (\sigma_a)_{bending} + (K_f)_{axial} \frac{(\sigma_a)_{axial}}{0.85} \right]^2 + 3 \left[(k_{fs})_{torsion} (\tau_a)_{torsion} \right]^2 \right\}^{1/2}$$

(7)

$$\sigma'_m = \left\{ \left[(K_f)_{bending} (\sigma_m)_{bending} + (K_f)_{axial} (\sigma_m)_{axial} \right]^2 + 3 \left[(k_{fs})_{torsion} (\tau_m)_{torsion} \right]^2 \right\}^{1/2}$$

(8)

The most of S-N curves are from tests where the mean stress was zero. Even though, the mean stress is commonly not zero when operating

under service conditions. Several basic engineering methods have been put forth to predict fatigue behavior when the stress cycles around mean stress. In our experimental tests, we used Soderberg's criteria. This equation is often preferred because using Soderberg adds a margin of safety higher from the other criterions based on yield strength [12,13].

$$\sigma'_a = \sigma_N \left[1 - \left(\frac{\sigma'_m}{\sigma_y} \right) \right]$$

(9)

Where: σ_N is the fatigue strength for N number of cycles.

σ'_a is the fatigue amplitude stress under condition of mean stress σ'_m

σ_y is the yield strength of the material.

The curve equation used to calculate the number of cycles N, where a and b were acquired experimentally curve.

$$\sigma_N = aN_f^b$$

(10)

4- Results:

4-1. Tensile results:

The experimental results for the tensile test in each case were represented in stress-strain curves shown in Fig. 4. Nitinol has a higher stress resistance at room temperature than at (0°C) and a lower value at (-20°C), where the yield strengths were (849.32, 578.66, and 304.59) MPa respectively.

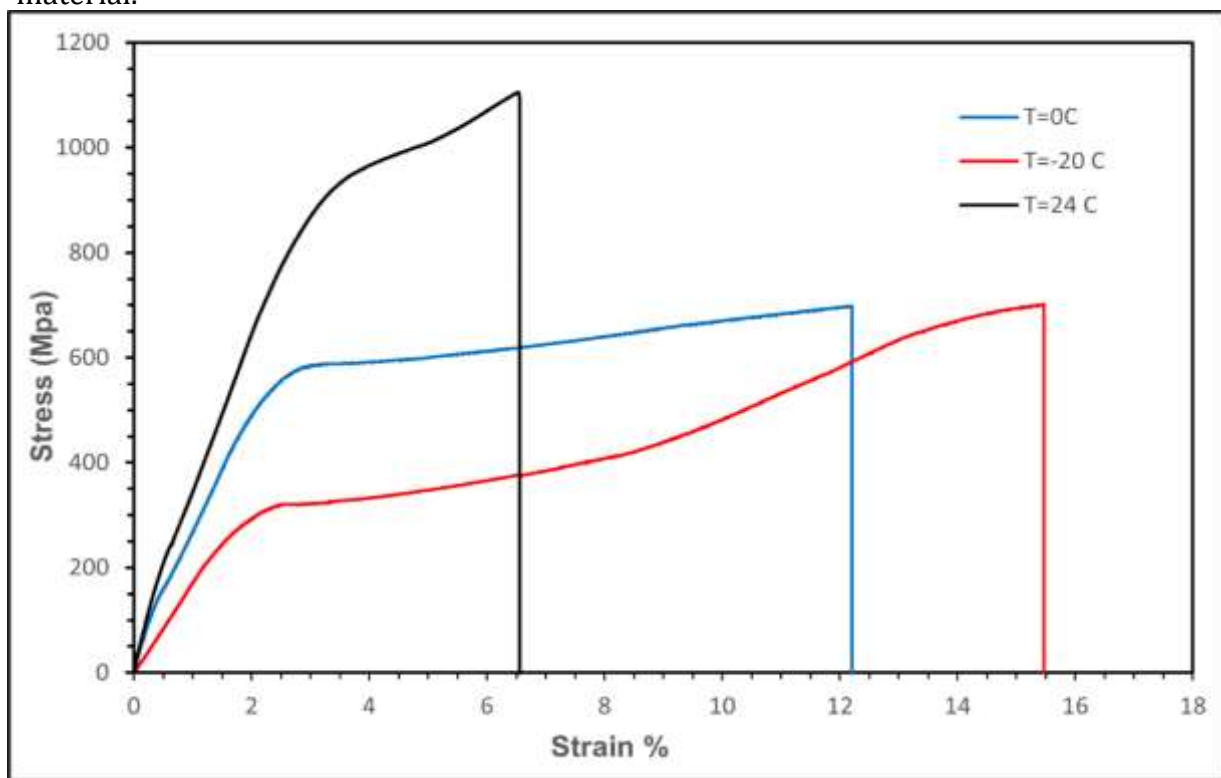


Fig. 4. Tensile stress-strain curves for nitinol in three different test temperatures

Materials are intended to become brittle as the temperature drops, but as we can see, nitinol acts in quite a different manner. That is because shape memory alloys undergo a reversible phase transformation called martensitic transformation, which is responsible for its shape memory properties. At low temperatures, nitinol exists in a martensite phase, which is relatively soft and has lower strength. At higher temperature, it will be in the austenite phase, which is a higher temperature phase with higher

strength. As previously mentioned for the nitinol samples used in this work, the austenite start temperature (A_s) is (-2°C) and the austenite finish temperature (A_f) is (10°C), so the test at (24°C) is expected to be at a temperature higher than the martensitic deformation temperature (M_d), at which nitinol behaves like a conventional metal in tensile tests because the martensitic transformation in nitinol is temperature-dependent, and it typically occurs when the material is subjected

to stress at temperatures below its M_d temperature, so, the phase change is suppressed at this degree [14]. This means that nor thermal or stress-induced martensite is present in this instance. When the temperature falls to zero, the temperature below (M_d) and the tension stress being applied lead to stress-induced martensite being created as a result of the stress, which reduces the strength and the modulus of elasticity compared to the first scenario. In this situation, we are able to say that the alloy has a mixture of austenite and stress-induced martensite. At temperature test (-20°C) which is below the martensite start temperature, more of the nitinol transitions into the martensitic phase by the effect of temperature in addition to martensite induced by stress, that means the alloy will be in a completely martensite phase which led the strength and elastic modulus to be at the lowest values.

4-2: Fatigue results:

The fatigue test findings, indicating the amount of stress applied to the sample during each test and the number of cycles at which the sample broke under that stress, are shown by the semi-log S-N curve in Fig. 5. The first thing we can

notice is that all three curves fall into the high-cycle fatigue region ($N > 1000$ cycles), this is because the applied stresses in the tests were selected near the yield strength of the material. We note that the relationship between the applied load and the needed number of failure cycles as usual in fatigue tests is an inverse relationship. The specimen fails at fewer cycles as the load increases. We see that the specimens tested at 0°C required fewer loading cycles before failing than those tested at 24°C , whereas the samples tested at -20°C failed after the fewest loading cycles. For each scenario, the following fatigue life equations were obtained from the S-N curve:

For test temperature ($T=24^\circ\text{C}$),
 $\sigma_a = 1581.8N^{-0.08}$ (11)

For test temperature ($T=0^\circ\text{C}$),
 $\sigma_a = 1769.9N^{-0.102}$ (12)

For test temperature ($T=-20^\circ\text{C}$),
 $\sigma_a = 1497.6N^{-0.125}$ (13)

The fatigue behavior of Nitinol can be influenced by temperature due to the changes in its microstructure and phase transformations.

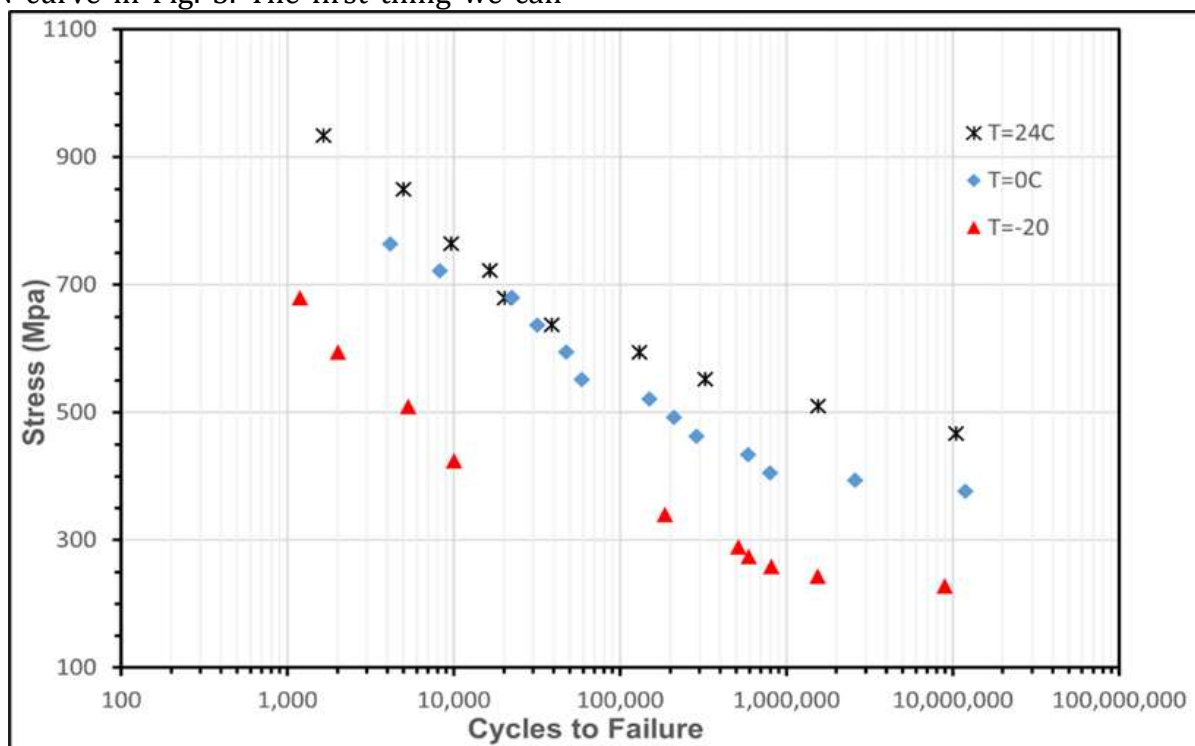


Fig. 5. Nitinol S-N curves at different test temperatures

5- Discussion of results:

Explaining the phase's crystal structure will help us determine why martensite can be so

elastic in tensile test. In the martensite phase, the atoms are arranged in the form of a centrally sized quadrilateral (a body-centered tetragonal) of 9 atoms distributed in the form of 8 in the corners of the structure and one in its center. This crystalline structure is less symmetrical and more flexible, as it is not crowded with atoms. Therefore, when subjected to external stress, this crystalline phase allows the material to form, as the atoms change their position easily according to a mechanism called (a detaining mechanism) converting twinned martensite into detained martensite. This process in martensite can result in a higher apparent elasticity which can withstand the maximum elongation due to its parallelogram structure. While in the austenite phase, the atoms are arranged in the form of a face-centered cube of 14 atoms (8 in the corners of the structure and one in the center of each face). Since austenite's crystal structure is symmetrical and compact (full of atoms), it exhibits relatively high resistance to external stress while keeping its original crystal structure [15]. The above-mentioned conclusions are in agreement with Melton and Mercier's work quite well [16]. Where two nitinol samples, $Ni_{49.9}Ti_{50.1}$ ($A_f=10^\circ\text{C}$) and $Ni_{49.7}Ti_{50.3}$ ($A_f=110^\circ\text{C}$), tested under uniaxial tensile stress at room temperature. The two samples were respectively at austenite and thermal martensite phases at test conditions. The results showed that the first composition had a higher stress plateau (corresponding to stress induced martensite formation) than the thermal martensite structure (corresponding to martensite detwinning and deformation), and the elastic modulus of the austenite is also higher than that of the martensite. We note that the percentage of deformation to failure increased as the test temperature dropped and that the maximum strain value is (15.4%) at a temperature of (-20°C), because the increase in martensitic content causes the alloy to become more flexible. Where, according to (Matt Reinhoehl) study, the stress required to deform thermal martensite is lower than those required to stress induce martensite under superelastic conditions [17]. Also, when nitinol undergoes the phase transformation from austenite to

martensite, it exhibits transformation-induced plasticity (TRIP). This means that during the phase transformation, the material undergoes a change in volume, leading to the accommodation of strain[18]. The value of the modulus of elasticity is also reduced with a decrease in test temperature, because the more disordered and defect-rich structure of martensite results in decreased bond strengths and increased atomic mobility, leading to a lower modulus of elasticity compared to austenite.

The observed results in the fatigue tests of Nitinol at different temperatures can be explained as follows:

Specimens tested at 0°C required fewer loading cycles before failing than those tested at 24°C . The reason is that when the test temperature is lowered to 0°C , the material's strength tends to decrease and they have reduced resistance to crack propagation. This means that cracks in the material can grow and propagate more easily, leading to a shorter fatigue life. The other reason is the effect of Stress-Induced Transformation. During cyclic loading, the stress levels experienced by the material can lead to stress-induced transformations between austenite and martensite phases. These transformations can create local areas of varying mechanical properties, potentially leading to crack initiation and reduced fatigue life in the martensite phase. Also, at lower temperatures, specimens experienced a reduction in their ability to dissipate heat generated during cyclic loading, resulting in a temperature difference between the sample's outer surface and its core which has accelerated failure by causing microscopic cracks to form on the outside surface. which can further contribute to reduced fatigue life. Additionally, the thermal stress effects. Temperature variations can induce thermal stresses in the material, particularly when cyclic loading is applied. These thermal stresses can interact with applied mechanical stresses, leading to complex stress distributions and potentially accelerating fatigue crack initiation and propagation. Samples tested at -20°C failed after the fewest loading cycles because the testing at even lower temperatures

exacerbates the issues mentioned above. The material becomes even more susceptible to crack growth and failure under cyclic loading. In addition to the effect of phase transformation expected in this case. As nitinol undergoes a phase transformation from austenite to martensite, it typically involves a change in crystal structure and shape. The phase transformation process can create stress concentrations and localized strain gradients in the material, which can act as initiation sites for fatigue cracks. In the case of martensite specimens, the repeated phase transformation during cyclic loading may lead to crack nucleation and accelerated crack growth, resulting in a shorter fatigue life compared to the austenite samples. In summary, the behavior of nitinol in fatigue testing is strongly

influenced by temperature due to its unique properties. Lower temperatures tend to reduce the effectiveness of these properties, leading to decreased fatigue life and premature failure. Conversely, testing at higher temperatures may provide better fatigue performance due to improved energy dissipation capabilities in the material. As such, the temperature range at which nitinol components are operated is an important consideration in their design and performance assessment.

With a little of deviation, the results of the actual experiments were in good accord with what was predicted by theoretical terms, as shown in Fig. 6. Where we observe that, with a few exceptions, the estimated number of cycles before failure is, on average, a little bit higher than the number that was actually recorded.

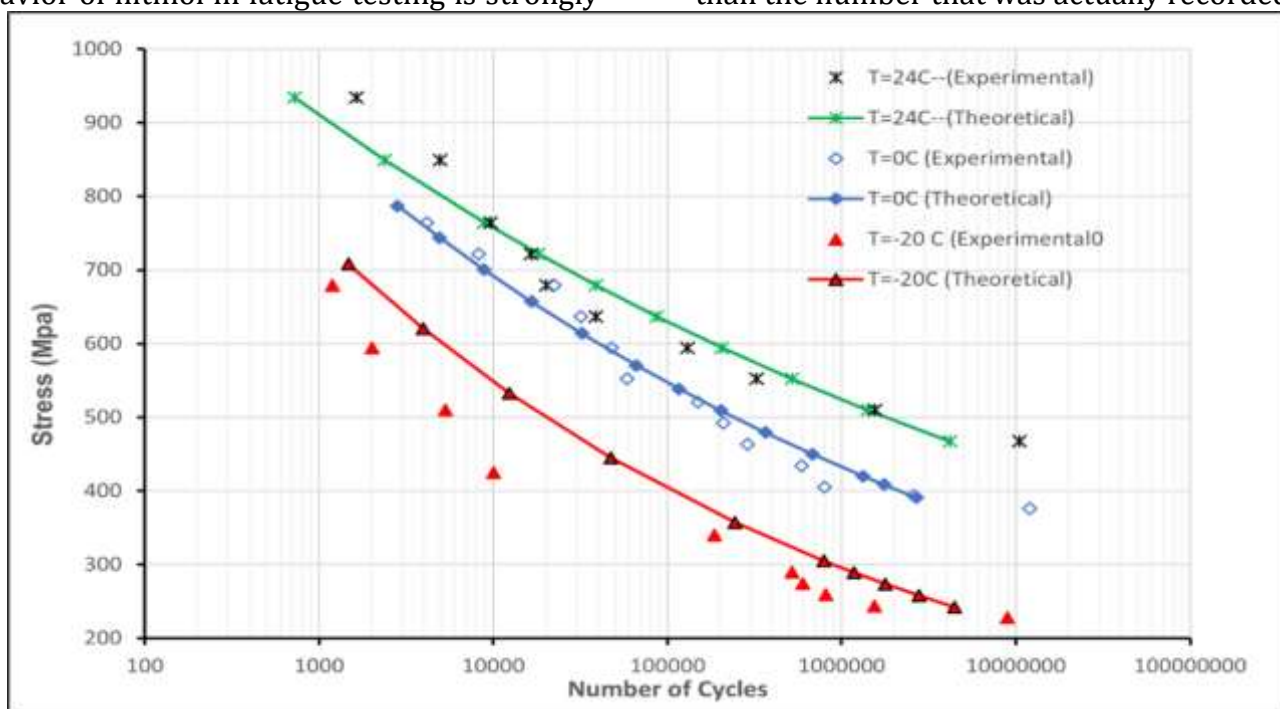


Fig. 6. Nitinol theoretical and experimental S-N curves in different temperature

Differences between experimental and theoretical results in fatigue testing can occur due to various reasons including microstructure, grain size, inclusions, and surface conditions such as surface roughness, and the presence of notches or scratches. Also, the effect of residual stresses which introduced during manufacturing processes, and affect the material's fatigue behavior. The variation in all these factors may not be fully accounted for in theoretical models (which often assume

idealized, uniform materials), but can significantly impact fatigue behavior and lead to differences between the theoretical assumptions and experimental results.

The ANSYS Workbench program (version 2019) was employed to simulate the fatigue life of specimens. After providing all necessary parameters from experimental work or earlier studies, the appropriate type of analysis—fatigue analysis utilizing Von Mises stress theory and Soderberg fatigue life type was chosen. the

repeated procedures show the corresponding fatigue life for each value of stress. Fig. 7. illustrates how the analytical simulation results and the research's actual results were in good

agreement. Several examples of equivalent von Mises stresses and life calculations from the simulation process are shown in Fig. 8. and Fig.9. respectively.

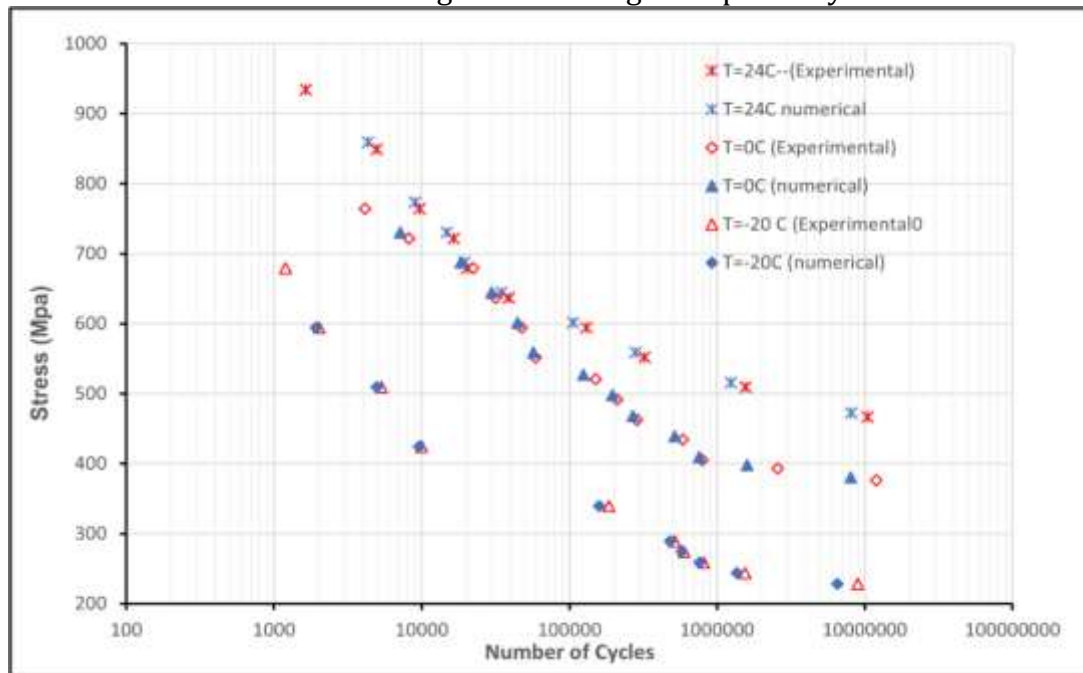


Fig. 7. An overview on numerical and experimental fatigue results

6- Conclusion:

The environment's temperature significantly impacts how shape memory alloys behave, when loaded under low-temperature conditions and the effects of temperature change depends on the type of alloy worked with and its phase transformation temperatures. No matter what kind of stress is applied (bending or tensile), a phase shift happens if the ambient temperature exceeds the alloy's phase transition temperatures. Tensile loading was clearly impacted by the phase change; the lowest yield stress value was noted at the coldest temperature, while its maximum level has been detected at room temperature. Due to the martensitic phase's crystalline structure, the largest value of elongation was measured at the lowest temperature utilized in the research. The crystalline structure of the phase transformation showed a lesser effect on the shape memory alloy's fatigue behavior than

yield strength, where martensite displayed lower resistance to continuous loading because the applied stress was higher than the yield stress. Since the ductility of martensitic over austenite increased when nitinol was operated at low temperatures that caused a phase shift, we conclude that this transformation did not support fatigue behavior under continuous loading. As a result, we advise using an alloy with a wider range of phase transition degrees when using nitinol for low-temperature applications to ensure the continuity of the austenite phase, which is it gives the highest strength. By controlling the chemical composition and applying the required heat treatments, an alloy can be made that is more homogenous and has a longer fatigue life. the analytical simulation produced results that were reasonably close to the practical experiments. so, it can be relied to conduct further analysis for different test temperatures.

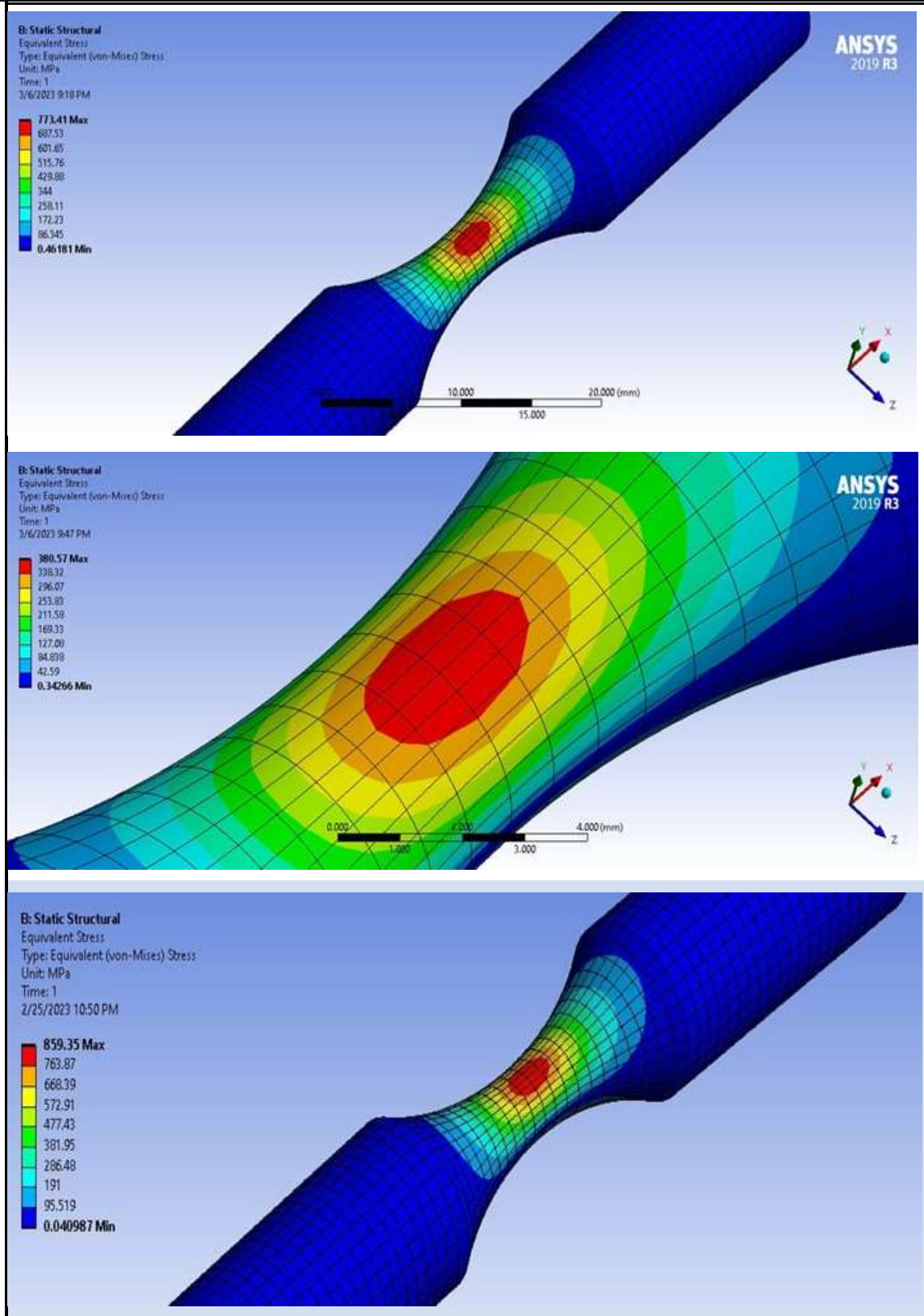


Fig. 8. Equivalent von Mises stresses for different samples simulations

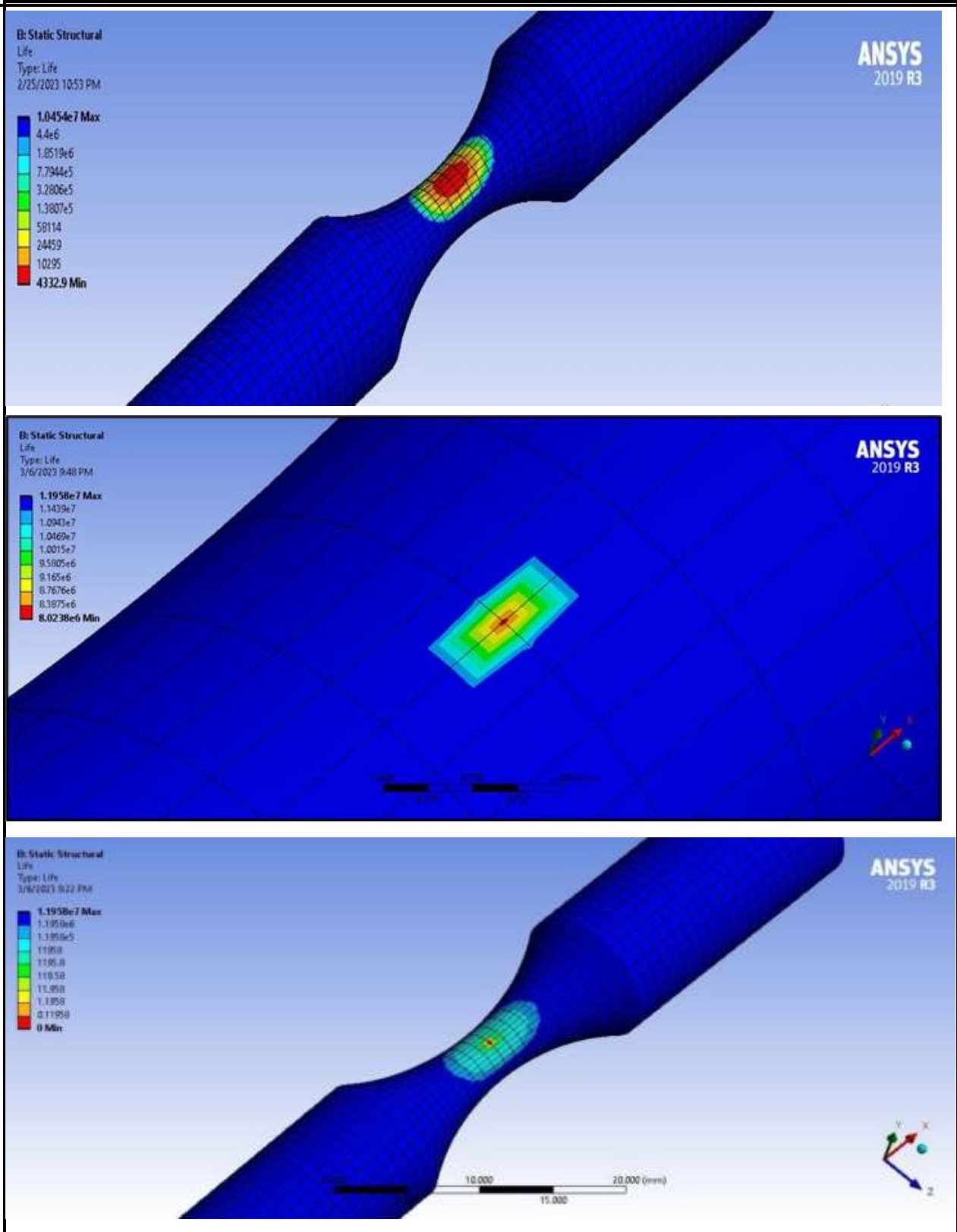


Fig. 9. Life Simulink for different fatigue samples

References:

1. M. H. Wu, P. Motzki, and S. Seelecke, "Industrial Applications for Shape Memory Alloys," *Encycl. Smart Mater.*, vol. 182, no. January, pp. 254–266, 2021,

- doi: 10.1016/B978-0-12-803581-8.11723-0.
2. Ai A. Aljebouri¹, S. H. Mohammed² * M. A. Mohammed³, "Effect of Sn Addition on Phase Transformation Behavior of

- Equiatomic Ni-Ti Shape Memory Alloy “, Baghdad Science Journal, 2020, 17(3) Supplement (September):961-966.
3. V. V Vasiliev and E. V Morozov, *Mechanics and analysis of composite materials*. Elsevier, 2001.
 4. R. I. Stephens, *Fatigue at low temperatures: a symposium*, no. 857. ASTM International, 1985.
 5. X. Chen, K. Liu, W. Guo, N. Gangil, A. N. Siddiquee, and S. Konovalov, “The fabrication of NiTi shape memory alloy by selective laser melting: a review,” *Rapid Prototyp. J.*, vol. 25, no. 8, pp. 1421–+31432, 2019, doi: 10.1108/RPJ-11-2018-0292.
 6. A. Abdulrusool, S. J. Mosa, “The Effective of Pressure and Sintering Temperature for Hardness Characteristics of Shape Memory Alloy by Using Taguchi Technique”, *Journal of Engineering*, NO. 1, Vol. 22, January 2016.
 7. M. Balasubramanian, R. Srimath, L. Vignesh, and S. Rajesh, “Application of shape memory alloys in engineering - A review,” *J. Phys. Conf. Ser.*, vol. 2054, no. 1, 2021, doi: 10.1088/1742-6596/2054/1/012078.
 8. Z. Alfay, A. M. Takhakh, A. K. Abid-Ali, “Effect of Nb Addition on Hardness and Wear Resist of Cu-Al-Ni Shape Memory Alloy Fabricated by Powder Metallurgy”, *Journal of Engineering*, No. 1 Vol. 20 January 2014.
 9. T. Ikeda, *The use of shape memory alloys (SMAs) in aerospace engineering*, no. iii. Woodhead Publishing Limited, 2011. doi: 10.1533/9780857092625.2.125.
 10. J. Uchil, K. P. Mohanchandra, K. G. Kumara, K. K. Mahesh, and T. P. Murali, “Thermal expansion in various phases of Nitinol using TMA,” vol. 270, pp. 289–297, 1999.
 11. Richard G. Budynas, J. Keith Nisbett. (2011). “ Shigley’s Mechanical Engineering Design”, Ninth Edition. (McGraw-Hill series in mechanical engineering).
 12. E. J. HEARN. (2000). “MECHANICS OF MATERIALS”. Third Edition. (Butterworth Heinemann Linacre House, Jordan Hill, Oxford OX2 8DP).
 13. Alalkawi H. J. M, Ali Yousuf Khenyab, Abduljabar H. Ali “Improvement of Mechanical and Fatigue Properties for Aluminum Alloy 7049 By Using Nano Composites Technique”, *Al-Khwarizmi Engineering Journal*, Vol. 15, No. 1, March, (2019), P.P. 1- 9.
 14. D. Arau, A. Daniel, D. O. Ramos, C. Jose, G. A. Mace, and C. Jose, “An experimental investigation of the superelastic fatigue of NiTi SMA wires,” vol. 0, 2018, doi: 10.1007/s40430-018-1101-0.
 15. J. C. Chekotu, R. Groarke, K. O’Toole, and D. Brabazon, “Advances in selective laser melting of Nitinol shape memory alloy part production,” *Materials (Basel)*., vol. 12, no. 5, 2019, doi: 10.3390/MA12050809.
 16. K. N. Melton and O. Mercier, “Fatigue of NITI thermoelastic martensites,” *Acta Metall.*, vol. 27, no. 1, pp. 137–144, 1979, doi: 10.1016/0001-6160(79)90065-8.
 17. A. Runciman, D. Xu, A. R. Pelton, and R. O. Ritchie, “The influence of melt practice on final fatigue properties of superelastic NiTi wires,” *Biomaterials*, vol. 32, no. 22, pp. 4987–93, 2011.
 18. Y. Zhang *et al.*, “Concentration of transformation-induced plasticity in pseudoelastic NiTi shape memory alloys: Insight from austenite-martensite interface instability,” *Int. J. Plast.*, vol. 160, no. July 2022, p. 103481, 2023, doi: 10.1016/j.ijplas.2022.103481.